Chapter 29
Enhanced Anti-stokes Raman Gain in Nonlinear Waveguides

A. D. Sanchez[1,4], S. M. Hernandez[2], J. Bonetti[2,3], D. F. Grosz[3], and P. I. Fierens[4(✉)]

[1] Instituto Balseiro (IB), Bariloche, Argentina
alfredo.sanchez@ib.edu.ar
[2] IB, Bariloche, Argentina
[3] IB and Consejo Nacional de Investigaciones Científicas y Técnicas (CONICET), Buenos Aires, Argentina
[4] Instituto Tecnológico de Buenos Aires (ITBA) and CONICET, Buenos Aires, Argentina
pfierens@itba.edu.ar

Abstract. We show that, under certain conditions, modulation instability in nonlinear waveguides gives rise to the usual double-sideband spectral structure, but with a Raman gain profile. This process is enabled by the energy transfer from a strong laser pump to both Stokes and anti-Stokes sidebands in a pseudo-parametric fashion. We believe this striking behavior to be of particular value in the area of Raman-based sensors which rely on sensitive measurements of the anti-Stokes component.

29.1 Introduction

Pulse propagation in a lossless nonlinear waveguide is well described by the generalized nonlinear Schrödinger equation (GNLSE) [1]

$$\frac{\partial A(z,T)}{\partial z} - i\hat{\beta}A(z,T) = i\hat{\gamma}A(z,T)\int_{-\infty}^{\infty} R(T')\left|A(z,T-T')\right|^2 dT', \qquad (29.1)$$

where $A(z,T)$ is the slowly-varying envelope, z is the spatial coordinate, and T is the time coordinate in a comoving frame at the group velocity. $\hat{\beta}$ and $\hat{\gamma}$ are operators related to the dispersion and nonlinearity, respectively, and are defined by

$$\hat{\beta} = \sum_{m\geq 2} \frac{i^m}{m!}\beta_m \frac{\partial^m}{\partial T^m}, \qquad \hat{\gamma} = \sum_{n\geq 0} \frac{i^n}{n!}\gamma_n \frac{\partial^n}{\partial T^n}. \qquad (29.2)$$

β_m are the coefficients of the Taylor expansion of the propagation constant $\beta(\omega)$ around a central frequency ω_0. Similarly, γ_n are the coefficients of the Taylor

expansion of the nonlinear parameter. It is usually sufficient to consider the expansion up to the first term. Under this setting, it can be shown that the total number of photons is conserved if $\gamma_1 = \gamma_0/\omega_0$ [2], which is the usual approximation.

The function $R(T)$ models the Raman response of the medium. Stimulated Raman scattering is a non-parametric process that involves the excitation of molecular vibration modes of the waveguide and it does not conserve the energy of the wave. However, it does conserve the number of photons. Qualitatively speaking, the energy exchange experienced by a strong continuous-wave laser involves the annihilation of a pump photon and the simultaneous creation of another photon in a low-frequency (also known as Stokes) band. Similarly, a photon in a high-frequency (anti-Stokes) band is annihilated and another photon is created at the pump frequency. As a result, a *gain is observed only in the Stokes band*, enabling the application of stimulated Raman scattering in optical amplification [3].

First order linear perturbation analysis of the GNLSE reveals that, under certain conditions (*viz.*, anomalous dispersion), continuous-wave (CW) solutions are unstable. This phenomenon, known as modulation instability (MI) [4–11], is a parametric process where two photons from a CW pump are transferred to both low- and high-frequency bands, one photon each. As a result, *MI gain is observed in both sides of the pump*. It has been shown [12,13] that, when γ_1 is included, there is a power cutoff above which the MI gain vanishes.

In a recent work [14], we proved that there is still gain beyond the MI power cutoff when Raman scattering is taken into account. Moreover, we showed that the gain mimics the shape of the Raman response in the Stokes band. Here we extend these observations to the anti-Stokes band. Indeed, in the next section we show that there is *MI gain in both sides of the pump with a Raman spectral shape*. Further, we show this to be a pseudo-parametric process, that is, *a truly MI-like process where the anti-Stokes gain is not the result of one mediated by spectral generation in the Stokes band followed by four-wave-mixing generation in the anti-Stokes band*.

29.2 Raman and Modulation Instability

A few simulations may help to understand the behavior of stimulated Raman scattering. Figure 29.1 shows simulation results of an average over 50 noise realizations of a CW pump with additive white Gaussian noise. The signal was propagated a distance L_R, defined as the inverse of the peak Raman gain, in a normal dispersion regime. In particular, $\beta_2 = 50\,\mathrm{ps}^2/\mathrm{km}$, $\beta_m = 0$ for $m > 2$, $\gamma_0 = 100\,1/\mathrm{W/km}$, $\gamma_1/\gamma_0 = \omega_0^{-1}$. The pump power was set to $P_0 = 50\,\mathrm{W}$, its frequency to $\omega_0/2\pi = 376.73\,\mathrm{THz}$, and the signal-to-noise power ratio was 50 dB. For the Raman response [1], we used $R(T) = (1 - f_R)\,\delta(T) + f_R h_R(T)$, where f_R weights the contributions of the instantaneous (electronic) and delayed Raman response of the medium. We used the damped-oscillator approximation $h_R(t) \propto e^{-t/\tau_2} \sin(t/\tau_1)\,\Theta(t)$, where $\Theta(t)$ is the unit step function. We fixed $f_R = 0.031$, $\tau_1 = 15.5\,\mathrm{fs}$ and $\tau_2 = 230.5\,\mathrm{fs}$.

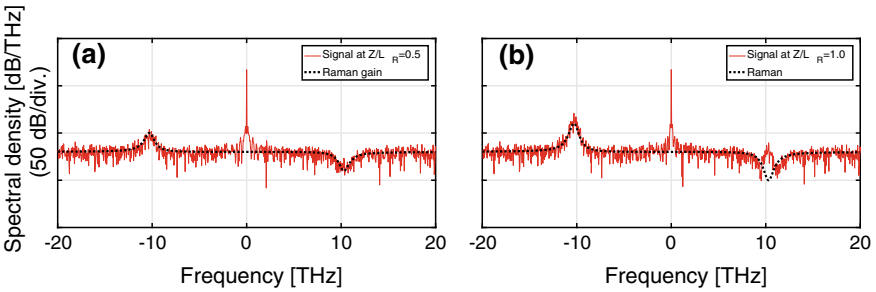

Fig. 29.1. Simulation results of an average over 50 noise realizations of a CW pump with additive white Gaussian noise: **a** at a propagated a distance $L_{\mathrm{R}}/2$; **b** at L_{R}. L_{R} is defined as the inverse of the peak Raman gain. The shape of the theoretical Raman gain (black dashed line) is also presented for comparison

Figure 29.1a shows the spectral density at $L_{\mathrm{R}}/2$, as a function of frequency deviations with respect to ω_0. We observe that noise in the Stokes band (negative frequencies) grows following the Raman gain as expected. However, in the anti-Stokes band noise decreases as photons are annihilated and new photons are created at the pump frequency. In Fig. 29.1b, after the signal propagates the remaining distance, it can be observed the growth of the anti-Stokes band through a third-order parametric process known as four-wave mixing (FWM). FWM involves the interaction between two pump photons with a Stokes and an anti-Stokes photon. In this sense, modulation instability (in the absence of Raman) is usually regarded as a four-wave mixing process.

A complete analysis of modulation instability includes the complex interplay between high-order dispersion, nonlinearity, and Raman scattering (see, e.g., [15,16]). For the sake of simplicity, let us consider the case where $\beta_m = 0$ for $m > 2$ and $\gamma_n = 0$ for $n > 1$. It can be shown that the MI gain is given by [17]

$$g_{\mathrm{MI}}(\Omega) = 2\max\{-\mathrm{Im}\{K_1(\Omega)\}, -\mathrm{Im}\{K_2(\Omega)\}, 0\}, \tag{29.3}$$

$$K_{1,2}(\Omega) = \frac{p|\beta_2|}{\tau}\Omega(1+\tilde{R}(\Omega)) \pm |\beta_2\Omega|\sqrt{\frac{\Omega^2}{4} - \frac{p\tilde{R}(\Omega)}{\tau^2} + \frac{p^2\tilde{R}^2(\Omega)}{\tau^2}}, \tag{29.4}$$

where Ω is the deviation from the pump frequency ω_0 and $\tilde{R}(\Omega)$ is the Fourier transform of the Raman response $R(T)$. For convenience, γ_1 and the pump power P_0 have been normalized as $\tau = \gamma_1/\gamma_0$ and $p = P_0/P_{\mathrm{c}}$, with

$$P_{\mathrm{c}} = \frac{|\beta_2|\gamma_0}{\gamma_1^2}. \tag{29.5}$$

In the absence of Raman scattering, $\tilde{R}(\Omega) = 1$. In this case, it is easy to verify that there is no gain when $p > 1$, that is, when the pump power P_0 is beyond the power cutoff P_{c}. However, in the presence of Raman scattering ($\tilde{R}(\Omega) \neq 1$), there exists MI gain even for $p > 1$.

In order to understand the nature of the processes involved, it is convenient to study the number of photons, a quantity conserved when $\tau = \omega_0^{-1}$, as it was already explained. Let us define the quantity

$$\Psi(\Omega) = \frac{|A(z,\Omega)|^2}{\hbar\,(\Omega + \omega_0)}, \tag{29.6}$$

which is proportional to the number of photons at frequency Ω. Figure 29.2a shows simulation results for the propagation of a pump and two seeds located at the Stokes and anti-Stokes frequencies (∓ 10.7 THz) under the same setting as that of Fig. 29.1 (both seeds have the same number of photons at $z = 0$.) It is observed that initially the number of photons at the anti-Stokes frequency decreases as a consequence of Raman scattering, and then begins to increase (at a distance $z \sim 0.4\,L_{\mathrm{R}}$) due to FWM. Figure 29.2b–c show the evolution of the same quantity in a purely parametric process such as MI in the absence of Raman. The normalized pump power is $p = 0.8$, the fiber dispersion is anomalous, $\beta_2 = -50\,\mathrm{ps}^2/\mathrm{km}$, and γ_0 and ω_0 are as in Fig. 29.1. The propagated distance is the characteristic MI length, defined as $L_{\mathrm{MI}} = \max(g_{\mathrm{MI}}^{-1})$. In Fig. 29.2b, $\gamma_1 = 0$ and, given that the number of photons is not conserved, seeds grow unevenly. On the contrary, in Fig. 29.2c, $\gamma_1 = \gamma_0/\omega_0$ and both seeds grow evenly.

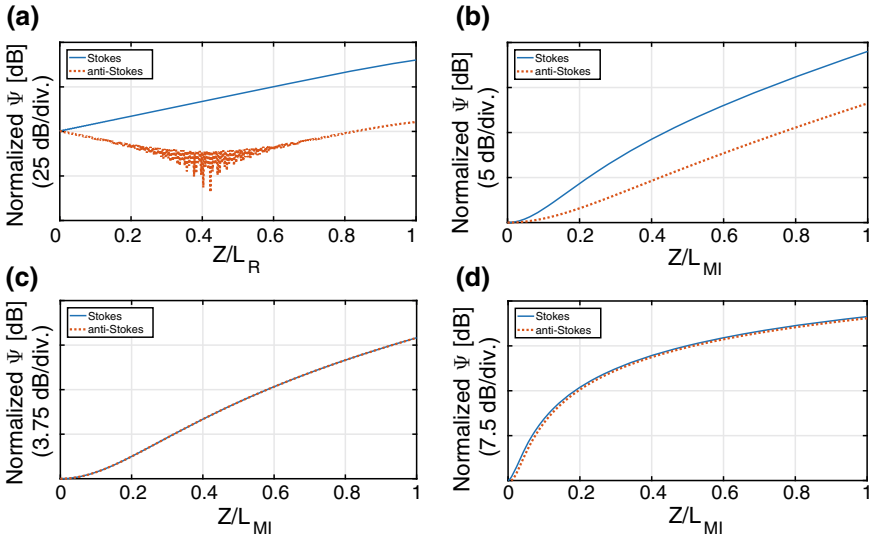

Fig. 29.2. Number of photons vs. normalized propagated distance for a pump and two seeds located at the Stokes and anti-Stokes frequencies (∓ 10.7 THz): **a** results for the normal dispersion regime; **b** anomalous dispersion regime with $p = 0.8$, $\gamma_1 = 0$ and no Raman scattering; **c** anomalous dispersion regime with $p = 0.8$, $\gamma_1 = \gamma_0/\omega_0$ and no Raman scattering; **d** anomalous dispersion regime with $p = 1.1$, $\gamma_1 = \gamma_0/\omega_0$ and Raman scattering

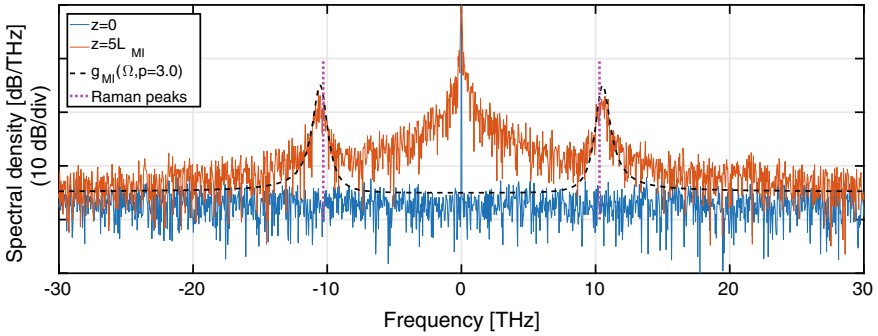

Fig. 29.3. Noise growth on the Stokes and anti-Stokes bands beyond the power cutoff ($p = 3.0$). Raman peaks at the Stokes and anti-Stokes at ∓ 10.7 THz are shown (dotted line). The MI-gain spectrum (black dashed curve) is also shown for comparison

If the effect of Raman scattering is included, MI gain cannot be the result of a purely parametric process. Recall Fig. 29.2a where the pump is shown to contribute photons only to the Stokes band, as it is the case with conventional Raman (non-parametric) amplification, and eventually the anti-Stokes band is amplified by means of a FWM interaction between the pump and the Stokes sideband. However, in the anomalous dispersion region of the waveguide, *we can have Raman amplification at both low- and high-frequencies simultaneously.* Indeed, Fig. 29.2d shows the evolution of both seeds for $p = 1.1$ and when Raman scattering is factored in. We observe that both seeds grow almost simultaneously (*cf.* Fig. 29.2a), and the slight difference in the growth rate is due to the actual gain of the Stokes band due to Raman. We may view the resulting behavior as intermediate between that of a purely parametric process, such as Fig. 29.2c, where the gain evolves simultaneously for low and high frequencies, and that of the Raman (non-parametric) gain in Fig. 29.2a.

Finally, in Fig. 29.3 the growth of noise shows clearly the amplification of both Stokes and anti-Stokes bands for $p = 3.0$ and after a propagated distance of $5\,L_{\mathrm{MI}}$. Although it is not evident from this figure, it can be shown that the gain spectra mimics the shape of the Raman response [14].

29.3 Conclusions

In this work we showed that beyond the modulation instability power cutoff nonlinear waveguides exhibit a gain with a Raman-like spectral shape. Inclusion of the higher-order nonlinear term γ_1 allows for the growth of both Stokes and anti-Stokes bands to be even and simultaneous, conserving the number of photons, as if in the presence of a pseudo-parametric process. As such, the nonlinear waveguide exhibits Raman gain in the anti-Stokes band, a striking feature that could find applications in the sensitivity enhancement of a wide variety of Raman sensors that rely on the monitoring of the anti-Stokes spectral component.

Acknowledgements. We gratefully acknowledge financial support from ONR Global through the Visiting Scientists Program.

References

1. G. Agrawal, *Nonlinear Fiber Optics*, 5th edn. Optics and Photonics (Academic Press, London, 2012)
2. K. Blow, D. Wood, IEEE J. Quantum Electron. **25**(12), 2665 (1989). https://doi.org/10.1109/3.40655
3. M. Ikeda, Opt. Commun. **39**(3), 148 (1981). https://doi.org/10.1016/0030-4018(81)90044-4
4. A. Hasegawa, W. Brinkman, IEEE J. Quantum Electron. **16**(7), 694 (1980). https://doi.org/10.1109/JQE.1980.1070554
5. K. Tai, A. Hasegawa, A. Tomita, Phys. Rev. Lett. **56**, 135 (1986). https://doi.org/10.1103/PhysRevLett.56.135
6. A. Demircan, U. Bandelow, Opt. Commun. **244**(1), 181 (2005)
7. J.M. Dudley, G. Genty, F. Dias, B. Kibler, N. Akhmediev, Opt. Express **17**(24), 21497 (2009). https://doi.org/10.1364/OE.17.021497
8. D. Solli, C. Ropers, P. Koonath, B. Jalali, Nature **450**(7172), 1054 (2007)
9. K. Hammani, C. Finot, B. Kibler, G. Millot, IEEE Photonics J. **1**(3), 205 (2009). https://doi.org/10.1109/JPHOT.2009.2032150
10. N. Akhmediev, J.M. Soto-Crespo, A. Ankiewicz, Phys. Rev. A **80**, 043818 (2009). https://doi.org/10.1103/PhysRevA.80.043818
11. S.T. Sørensen, C. Larsen, U. Møller, P.M. Moselund, C.L. Thomsen, O. Bang, J. Opt. Soc. Am. B **29**(10), 2875 (2012). https://doi.org/10.1364/JOSAB.29.002875
12. P.K. Shukla, J.J. Rasmussen, Opt. Lett. **11**(3), 171 (1986). https://doi.org/10.1364/OL.11.000171
13. C.D. Angelis, G. Nalesso, M. Santagiustina, J. Opt. Soc. Am. B **13**(5), 848 (1996). https://doi.org/10.1364/JOSAB.13.000848
14. A.D. Sánchez, S.M. Hernandez, J. Bonetti, P.I. Fierens, D.F. Grosz, J. Opt. Soc. Am. B **35**(1), 95 (2018). https://doi.org/10.1364/JOSAB.35.000095
15. P. Béjot, B. Kibler, E. Hertz, B. Lavorel, O. Faucher, Phys. Rev. A **83**, 013830 (2011). https://doi.org/10.1103/PhysRevA.83.013830
16. J. Bonetti, S.M. Hernandez, P.I. Fierens, D.F. Grosz, Phys. Rev. A **94**, 033826 (2016). https://doi.org/10.1103/PhysRevA.94.033826
17. S.M. Hernandez, P.I. Fierens, J. Bonetti, A.D. Snchez, D.F. Grosz, IEEE Photonics J. **9**(5), 1 (2017). https://doi.org/10.1109/JPHOT.2017.2754984